# QMC Studies of Quantum Nanowires and Nanolayers

**Neil D. Drummond and Richard J. Needs**

**TCM Group, Cavendish Laboratory, University of Cambridge**

*QMC in the Apuan Alps III, TTI, Vallico Sotto, Italy*

Monday 23rd July, 2007

# Quantum Nanowires and Nanolayers

- *Quantum nanowire* = 1D homogeneous electron gas.
- *Quantum nanolayer* = 2D homogeneous electron gas.
- QMC is the only accurate method for studying these systems.
- We have calculated / are calculating physically important quantities: binding energies, pair-correlation functions and structure factors.

# Quantum Nanowires (I)

- Experimental realisations of 1D HEGs: carbon nanotubes, Bechgaard salts, and one-dimensional channels etched on semiconductors.

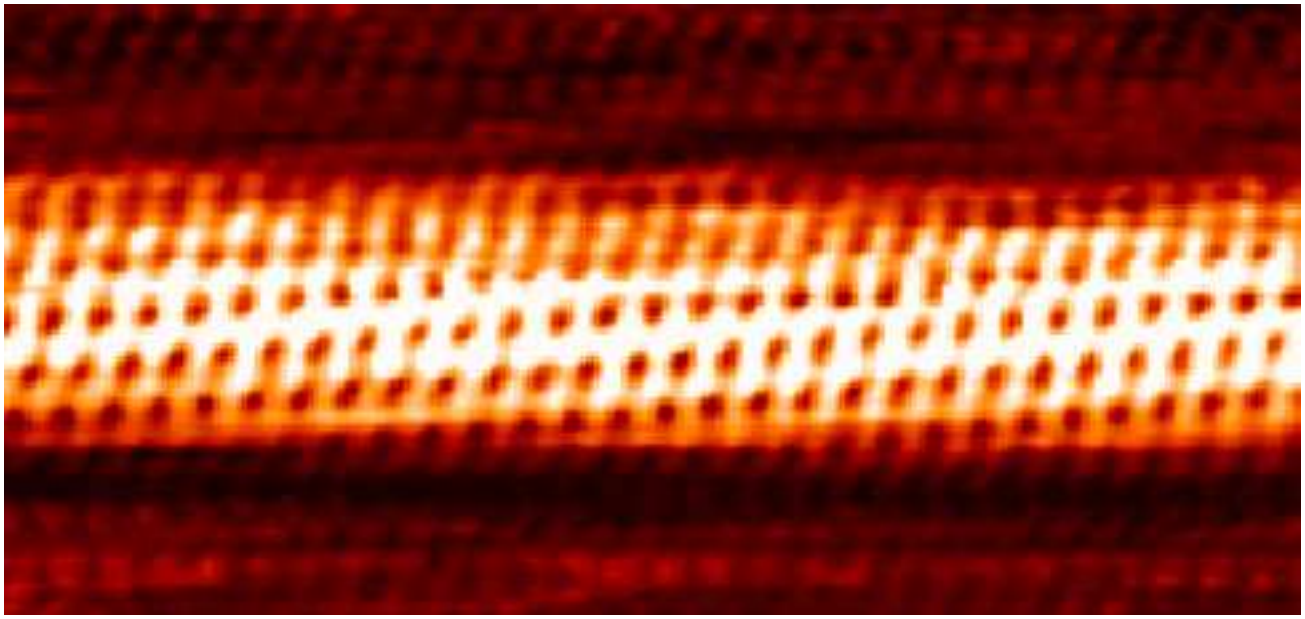

*STM image of a carbon nanotube*

- Rich variety of strongly correlated electron physics to explore.

# Quantum Nanowires (II)

- 1D HEG forms a strongly correlated *Luttinger liquid*,[1] not a Fermi liquid:
  - State of system immediately after the injection of an extra electron is orthogonal to the ground state (the *orthogonality catastrophe*).
  - $\delta$-function peak in the spectral function $A(k_F, \omega)$ at the chemical potential is not present, implying that single-electron quasiparticles are absent.
  - Forms insulator at zero temperature if any impurity is present due to the spontaneous formation of a charge-density wave.
  - Described (approximately) by the *Luttinger model*.

- Carbon nanotubes are important components of proposed nanotechnological devices.

- Carbon nanotubes attract by van der Waals interactions, but the asymptotic behaviour assumed in current models of nanotechnological systems may be wrong.

- Amazingly, the asymptotic form of van der Waals attraction between thin 1D conducting wires is controversial. We resolve the controversies using QMC.

[1] J. M. Luttinger, J. Math. Phys. **4**, 1154 (1963); F. D. M. Haldane, J. Phys. C **14**, 2585 (1981).

# One-Dimensional Coulomb Interactions

- We use the 1D effective Coulomb potential of Saunders *et al.*[2]

- For an electroneutral 1D system the Fourier coefficients of the Coulomb interaction are

$$\tilde{v}_{\mathbf{k}} = -\log(|\mathbf{k}|^2/4) - 2\gamma,$$

  where $\gamma$ is Euler's constant.

- All previous QMC studies[3] have used model interactions corresponding to a finite wire radius, thus avoiding the divergence at electron-electron coalescence points.

- For such interactions the Lieb-Mattis theorem (see later) implies that the ground state is paramagnetic.

- Our results correspond to the limit that the wire radius goes to 0: idealised limit.

---

[2] V. R. Saunders *et al.*, Comp. Phys. Comm. **84**, 156 (1994).

[3] A. Malatesta and G. Senatore, J. Phys. IV **10**, 5 (2000); Casula *et al.*, Phys. Rev. B **74**, 245427 (2006).

# Nodal Surface and Magnetic Behaviour (I)

- Consider 2 distinguishable particles of charge $q$ and $Q$ and mass $m$ and $M$, with relative position $x$. Hamiltonian:

$$\hat{H} = -\frac{1}{2\mu}\frac{d^2}{dx^2} + \frac{qQ}{|x|} + \hat{H}',$$

  where $\mu = mM/(m+M)$ is the reduced mass and $\hat{H}'$ does not depend on $x$.

- Suppose wave function is $\Psi = a_0 + \mathcal{O}(x)$.

- Suppose $a_0 \neq 0$. Then local energy

$$E_L = \frac{\hat{H}\Psi}{\Psi} = \frac{qQ}{|x|} + \mathcal{O}(x^0).$$

  This contains a nonintegrable divergence, so the energy expectation is undefined. Hence must have $a_0 = 0$. So $\Psi = 0$ at **all** coalescence points.

# Nodal Surface and Magnetic Behaviour (II)

- Hence the nodal surface is the set of points at which particles coincide.
- The nodal surface, and hence the fixed-node DMC energy, is independent of the spin polarisation.
- The 1D GS nodal surface is exact, so the DMC energies of 1D HEGs are exact.
- Therefore the GS energy of the 1D HEG is independent of the spin polarisation.
- Odd behaviour: if the charges are 0 then the ferromagnetic HEG is higher in energy than the paramagnetic HEG, but as soon as the charge is nonzero, paramagnetic and ferromagnetic energies are degenerate.
- Easiest way of getting nodal surface right: just work with ferromagnetic 1D HEGs.

# Nodal Surface and Magnetic Behaviour (III)

- Lieb–Mattis theorem[4]: consider a 1D Hamiltonian with a real, symmetric, *nonpathological* potential. If total spin $S' < S$ then GS energies satisfy $E_0(S') < E_0(S)$.

- However, 1D Coulomb interaction is pathological in the formal sense used by L&M: wave function is zero at points other than same-spin coalescence points (namely opposite-spin coalescence points).

- Weaker form of L–M holds if the potential is pathological: if $S' < S$ then $E_0(S') \leq E_0(S)$. So our conclusion that paramagnetic and ferromagnetic states are degenerate in energy does not contradict the L–M theorem.

- In real 1D systems the wire radius is finite, so that the electron–electron interaction is nonpathological. Hence real 1D systems will be paramagnetic by the L–M theorem.

[4] E. Lieb and D. Mattis, Phys. Rev. **125**, 164 (1062).

# Kato Cusp Conditions

- Let $x$ be the relative position of 2 indistinguishable particles of charge $q$ & mass $m$.
- Write $\Psi(x) = S(x)\exp[J(|x|)]$ where Slater part $S$ is analytic & odd in $x$. Then

$$\Psi(x) = [s_1 x + \mathcal{O}(x^3)]\exp[j_0 + j_1|x| + \mathcal{O}(|x|^2)] = [s_1 x + s_1 j_1 |x| x + \mathcal{O}(x^3)]\exp(j_0).$$

- Hence for $x > 0$

$$E_L = \Psi^{-1}\hat{H}\Psi = \left(\frac{-2j_1}{m} + q^2\right)x^{-1} + \mathcal{O}(x^0)$$

provided that $s_1 \neq 0$. Reach similar conclusion for $x < 0$.

- Hence must have $j_1 = mq^2/2$, i.e. $(\partial J/\partial|x|)_0 = mq^2/2$, to remove divergent term from $E_L$.

# Vandermonde Determinants

- 1D HEG Slater determinants are of Vandermonde form:

$$\Psi(x_1,\ldots,x_N) = \exp\left(-i\frac{\pi}{L}\sum_i\sum_{j\neq i}(x_i+x_j)\right)\begin{vmatrix} 1 & z_1 & z_1^2 & \cdots & z_1^{N-1} \\ 1 & z_2 & z_2^2 & \cdots & z_2^{N-1} \\ \vdots & & \vdots & & \\ 1 & z_N & z_N^2 & \cdots & z_N^{N-1} \end{vmatrix},$$

  where $z_i = \exp(2\pi i x_i/L)$, $N$ is the number of electrons and $L$ is the cell length.

- Could write the Slater determinant as a polynomial and evaluate it in a time that scales linearly with system size.

- Evaluating the 2-body Jastrow and backflow terms and the Coulomb potential is also slow, so have just used the standard determinant-updating machinery.

# Finite-Size Effects (I)

- Single-particle finite-size effects: shell filling causes discontinuous changes in the single-particle kinetic energy as the system size is increased at a given density.

- Periodic boundary conditions: $\Psi(x+nL) = \Psi(x)$ where $L$ is the simulation-cell length and $n \in \mathcal{Z}$. Single-particle orbitals are of the form $\exp(iGx)$ where $G = 2\pi n/L$.

- Twisted boundary conditions: $\Psi(x+L) = \exp(ik_tL)\Psi(x)$, where $-\pi/L < k_t < \pi/L$. Single-particle orbitals are of the form $\exp[i(G+k_t)x]$.

- Twist averaging: average over all $k_t \in (-\pi/L, \pi/L)$.

# Finite-Size Effects (II)

- Twist-averaged Hartree–Fock kinetic energy of $N$-electron 1D HEG:

$$\begin{aligned} T_N^{\mathrm{TA}} &= \frac{1}{N} \sum_{n=-\frac{N-1}{2}}^{\frac{N-1}{2}} \frac{L}{2\pi} \int_{-\pi/L}^{\pi/L} \frac{(2\pi n/L + k_t)^2}{2} \, dk_t \\ &= \frac{L}{2N\pi} \int_{-N\pi/L}^{N\pi/L} \frac{k^2}{2} \, dk = T_\infty, \end{aligned}$$

  so twist averaging completely removes single-particle finite-size effects in 1D.

- The Hartree–Fock exchange energy is independent of $k_t$ in 1D because the state occupancy is independent of $k_t$.

- Finite-size corrections due to truncation of long-ranged two-body Jastrow factor and compression of the exchange–correlation hole into simulation cell are still present.

# Hartree–Fock Theory for 1D HEG (I)

Hartree–Fock kinetic energy ($T$) and exchange ($X$) energies of 1D HEG:

$$
\begin{aligned}
T &= \frac{\pi^2}{192 r_s^2}\left[(1+\xi)^3+(1-\xi)^3\right] \\
X &= \frac{1}{8 r_s}\left\{(1+\xi)^2\left(\log\left[\frac{\pi(1+\xi)}{4r_s}\right]+\gamma-\frac{3}{2}\right)+(1-\xi)^2\left(\log\left[\frac{\pi(1-\xi)}{4r_s}\right]+\gamma-\frac{3}{2}\right)\right\}
\end{aligned}
$$

where $\xi$ is the spin polarisation and $\gamma$ is Euler's constant.

Hartree–Fock theory predicts a sharp transition from a paramagnetic fluid to a ferromagnetic one at $r_s = 2.191930959822221$ a.u.

# Hartree–Fock Theory for 1D HEG (II)

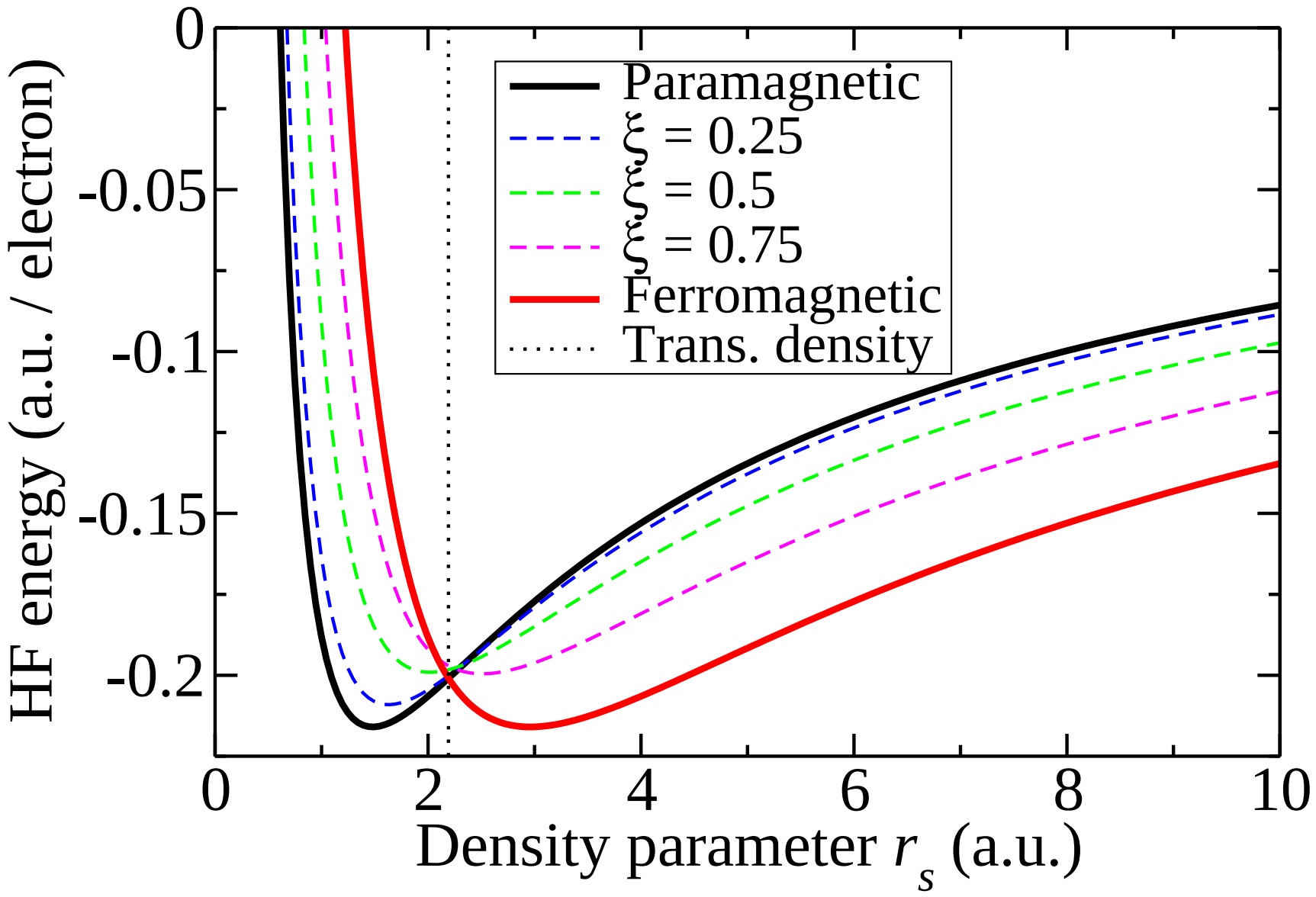

# Wire Energy Against Density (I)

- We use a ferromagnetic Slater wave function with plane-wave orbitals.
- Jastrow factor: two-body terms $(u + p)$ satisfying Kato cusp conditions.
- Backflow function: two-body term $(\eta)$ makes a significant improvement, even though the (already exact) nodal surface is not altered.
- Results for 15-electron wire at $r_s = 3$ a.u.:

| Method | Energy (a.u. per el.) | Variance (a.u.) | Percentage corr. energy |
|---|---|---|---|
| HF | $-0.215943040112$ | — | $0\%$ |
| SJ-VMC | $-0.2319668(4)$ | $0.0000360(2)$ | $99.974(3)\%$ |
| SJB-VMC | $-0.2319710(3)$ | $0.0000046(1)$ | $100.000(3)\%$ |
| SJB-DMC | $-0.2319709(3)$ | — | $100\%$ |

# Wire Energy Against Density (II)

- DMC energy suffers from very little time-step and population-control bias, because nodes are exact and trial wave function is so accurate.

- Use time steps of 0.04 a.u., 0.2 a.u. and 2.5 a.u. in our calculations at $r_s = 1$, 3 and 10 a.u., respectively and populations of 2048 configurations.

- Verified that energies do not change significantly when time step is halved; no need to extrapolate to zero time step.

- Carry out twist-averaged DMC calculations at different system sizes: randomly change twist angle then re-equilibrate every so often. (Not for binding-energy calculations.)

- Extrapolate to infinite system-size using

$$E_N^{\mathrm{TA}} = E_\infty + bN^{-3/2},$$

where $E_\infty$ and $b$ are determined by fitting. (Not for binding-energy calculations.)

# Binding Energy of a Biwire (I)

- Consider 2 parallel conducting nanowires (i.e. 1D HEGs, each with a neutralising line of background charge) with finite separation $z$.
- They are attracted to each other by van der Waals forces.
- Standard theory: van der Waals energy between wire elements $\delta l_1$ and $\delta l_2$ separated by $r$ is $\alpha \delta l_1 \delta l_2 / r^6$ where $\alpha$ is a constant.
- Current models of interacting carbon nanotubes etc. often use Lennard–Jones potentials [$U(r) = -A/r^6 + B/r^{12}$] to capture this long-range behaviour.[5]
- At wide separation the binding energy per particle is

$$U(z) = r_s \int_{-\infty}^{\infty} \frac{\alpha}{(x^2 + z^2)^3} \, dx \sim z^{-5}.$$

- Clearly appropriate for an insulator. What about a conductor?

[5] See L. A. Girifalco *et al.*, Phys. Rev. B **62**, 13104 (2000) and references thereto.

# Binding Energy of a Biwire (II)

- Recently-calculated binding energy per electron in the random phase approximation[6]:

$$U(z) \approx -\frac{\sqrt{r_s}}{16\pi z^2 \left[\log(2.39z/b)\right]^{3/2}}.$$

  where $b$ is the (finite) wire radius.

- RPA is believed to give the correct asymptotic form of binding energy, although the prefactor is approximate.

- Mean free path in carbon nanotubes can be $\sim$1 $\mu$m, much greater than the range of $z$ we study: impurities are not a problem.

- RPA may be invalid at low densities, where correlation effects become significant.

- Need an accurate first-principles method that can treat van der Waals effects. . . But we already know that QMC works for solid neon.[7]

[6] J. F. Dobson *et al.*, Phys. Rev. Lett. **96**, 073201 (2006).

[7] N. D. Drummond and R. J. Needs, Phys. Rev. B **73**, 024107 (2006).

# Binding Energy of a Biwire (III)

- Each wire has a neutralising background; need to add interaction between (a) electrons in wire 1 and background 2, (b) electrons in wire 2 and background 1 and (c) interaction between backgrounds 1 and 2.

- (a), (b) and (c) have same magnitude, but (c) has opposite sign. So, must subtract off electrostatic energy of a pair of parallel lines of the same charge. Hence must add $E_{\rm cap} = \log(z)/(2r_s)$ to our QMC energies.

- Perform biwire and monowire calculations with the same number of electrons per wire; finite-size errors should cancel. No need to twist average or add finite-size corrections.

- Expect results to be valid so long as separation is less than the simulation-cell size; after that system resembles a pair of insulating wires. Fit QMC data in range $r_s \ll z \ll N r_s$.

# Binding Energy of a Biwire (IV): $r_s = 1$ a.u.

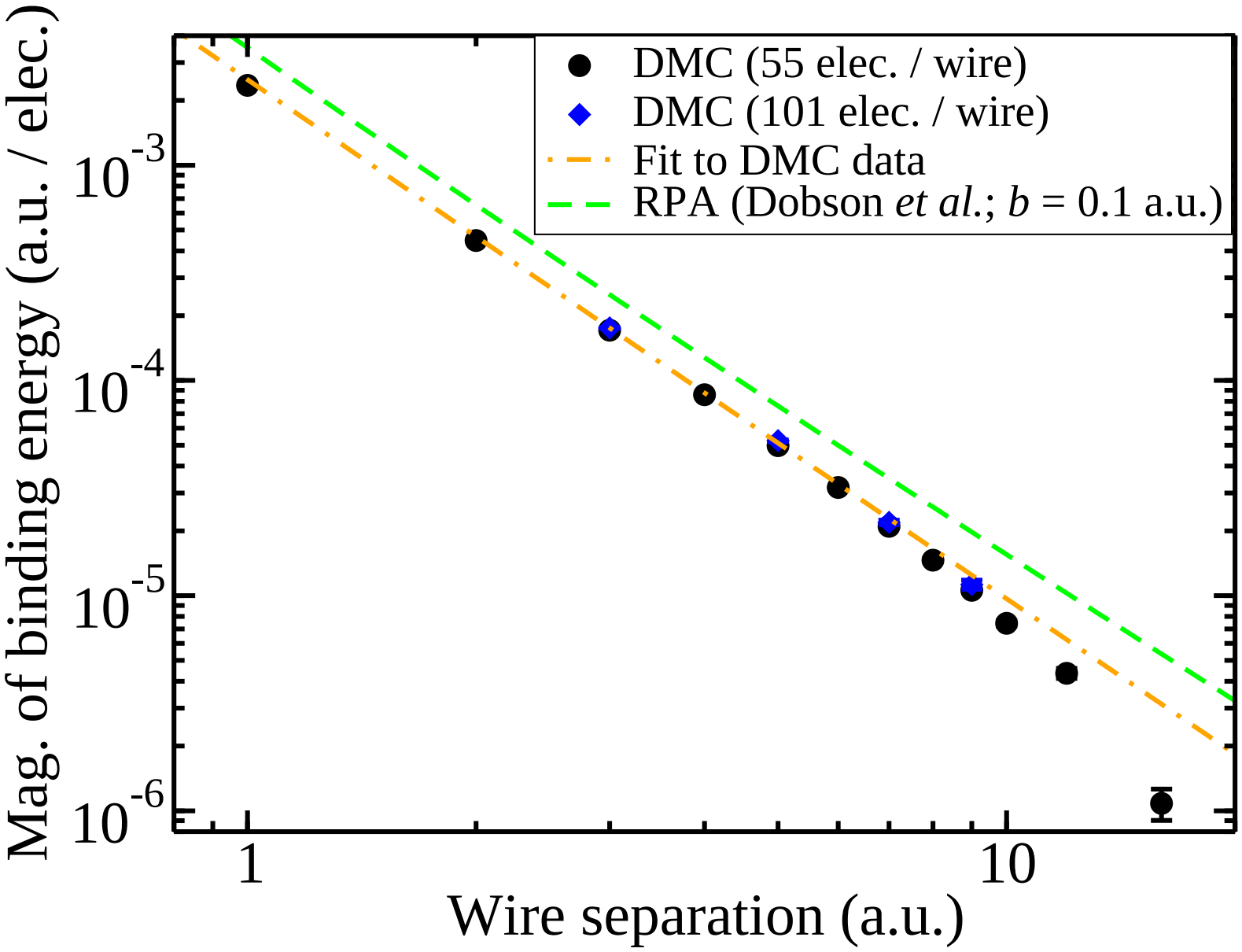

# Binding Energy of a Biwire (IV): $r_s = 3$ a.u.

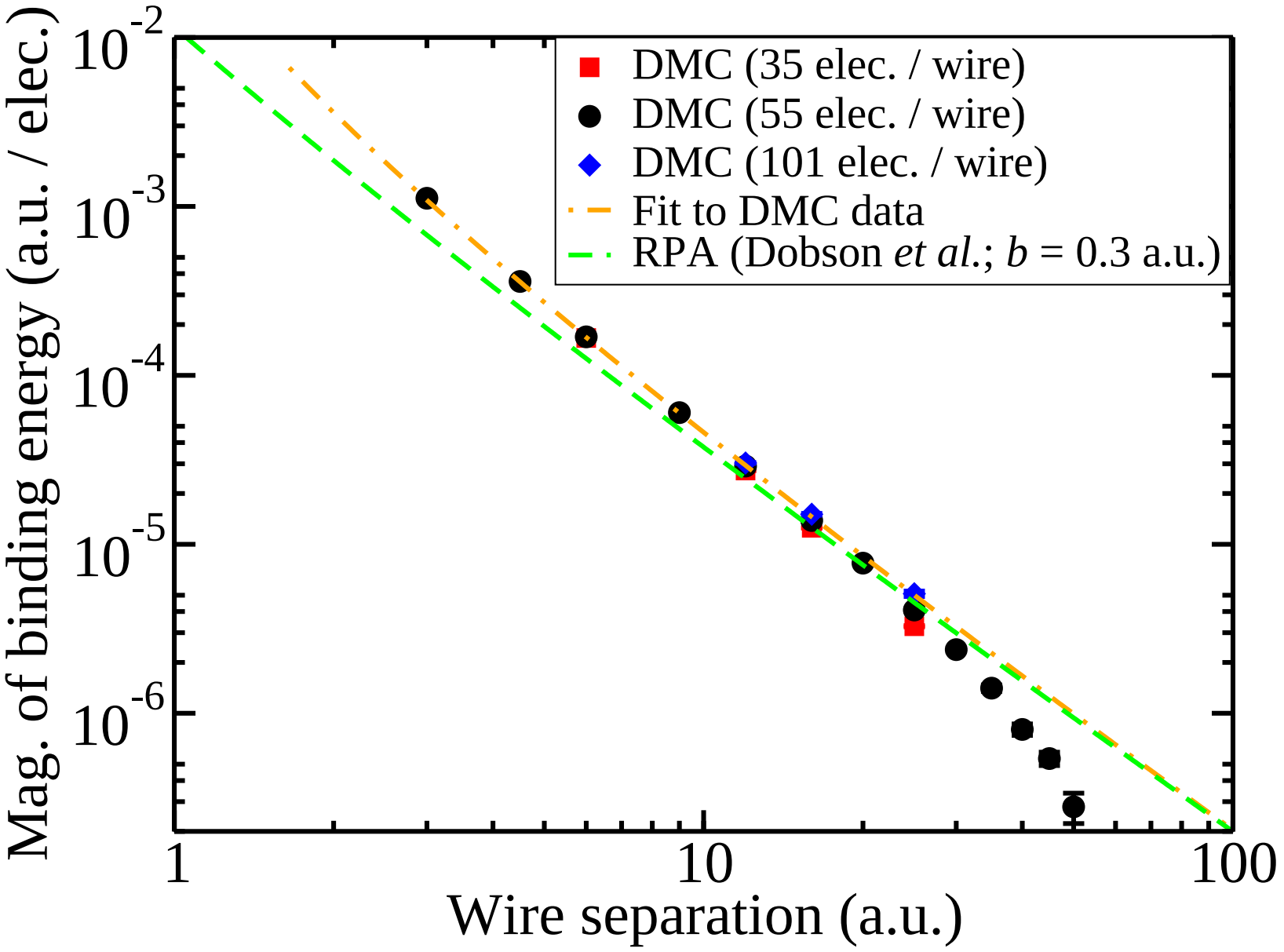

# Binding Energy of a Biwire (IV): $r_s = 10$ a.u.

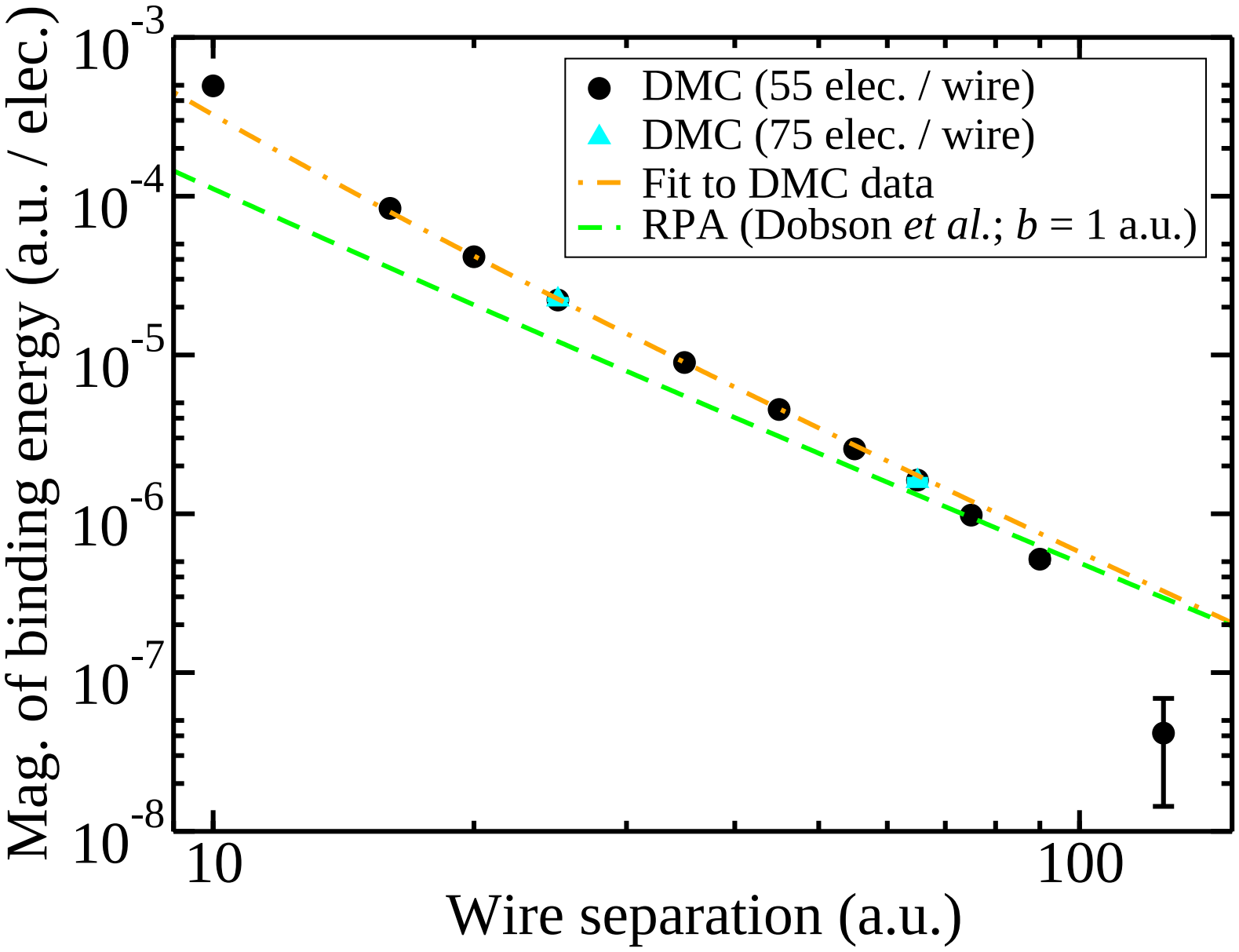

# Binding Energy of a Biwire (V)

| $r_s$ (a.u.) | Asymptotic binding energy (a.u. per electron) RPA | DMC |
|---|---|---|
| 1 | $-0.0199z^{-2}\left[\log(2.39z/b)\right]^{-3/2}$ | $-0.0815z^{-2.28}\left[\log(27000z)\right]^{-3/2}$ |
| 3 | $-0.0345z^{-2}\left[\log(2.39z/b)\right]^{-3/2}$ | $-0.0225z^{-1.98}\left[\log(1.95z)\right]^{-3/2}$ |
| 10 | $-0.0629z^{-2}\left[\log(2.39z/b)\right]^{-3/2}$ | $-0.0967z^{-2.17}\left[\log(0.492z)\right]^{-3/2}$ |

- The DMC binding energies are in broad agreement with the RPA predictions. They fall off much less rapidly than the $z^{-5}$ decay predicted by the standard theory.

- It is not meaningful to compare the prefactors because the RPA expression is not valid in the limit that $b \longrightarrow 0$.

- Uncertainties in exponents are about $0.1$–$0.2$.

# Wire and Biwire Pair-Correlation Functions (I)

- Accumulate PCF $g(x)$ by binning interparticle distances during QMC simulation.
- Errors in $g_{\mathrm{VMC}}(x)$ and $g_{\mathrm{DMC}}(x)$ are 1st order in error in trial wave function, but error in $g_{\mathrm{Ext}}(x) = 2g_{\mathrm{DMC}}(x) - g_{\mathrm{VMC}}(x)$ is 2nd order in error in wave function.
- There are long-ranged oscillations in the PCF. Tail of PCF is (probably)

$$g(x) = 1 + A \exp\left(-b\sqrt{\log|x/c|}\right) \cos(2k_F x),$$

  where $A$, $b$ and $c$ are fitting parameters and $k_F = \pi/(2r_s)$ is the Fermi wave number.
- Fit tail to QMC data, to extend PCF beyond simulation cell.
- Correlation hole in interwire PCF is tiny. Accurate interwire PCF data needed to construct van der Waals energy functionals for 1D systems.

# Wire and Biwire Pair-Correlation Functions (II)

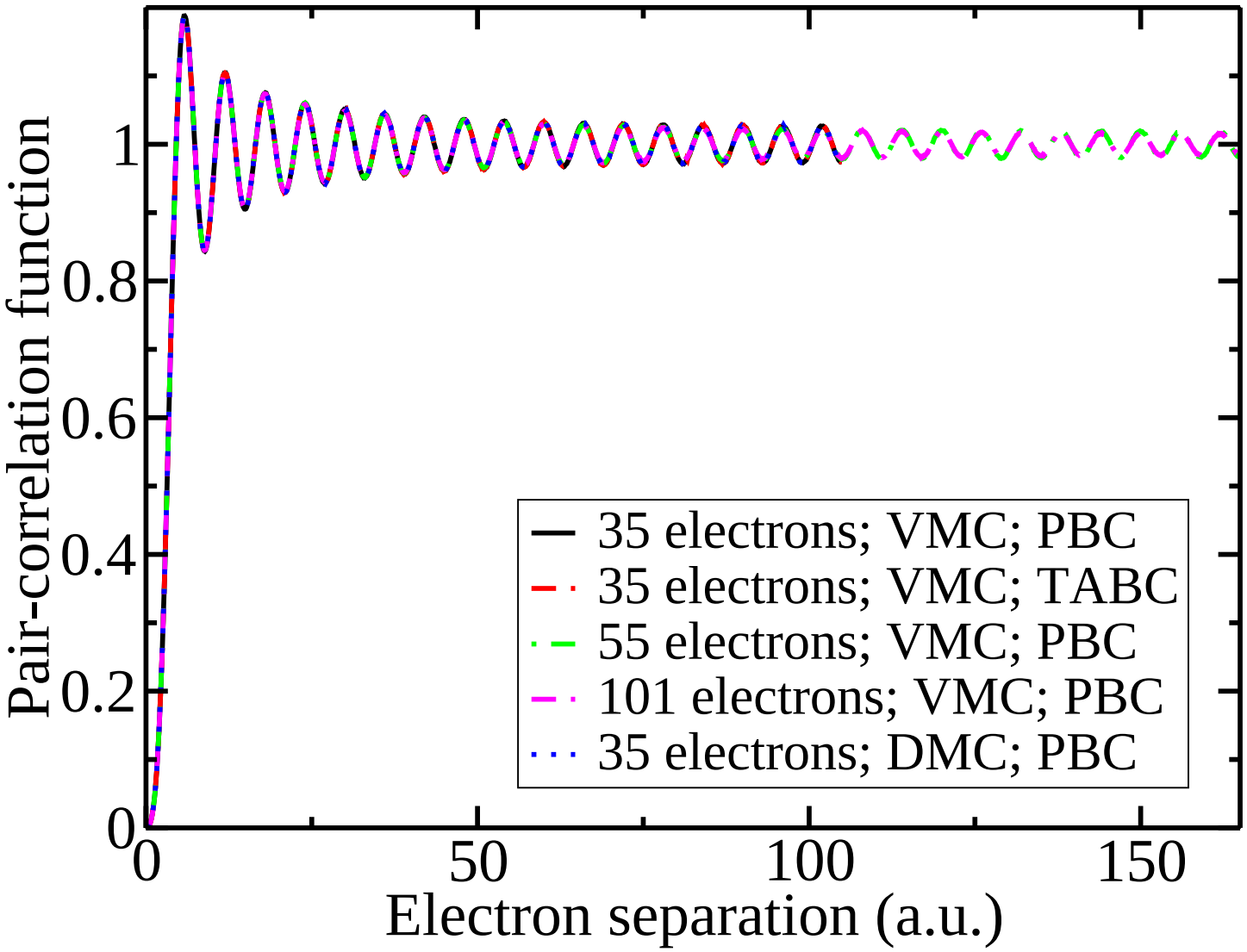


$r_s = 3$ a.u.

# Wire and Biwire Pair-Correlation Functions (III)

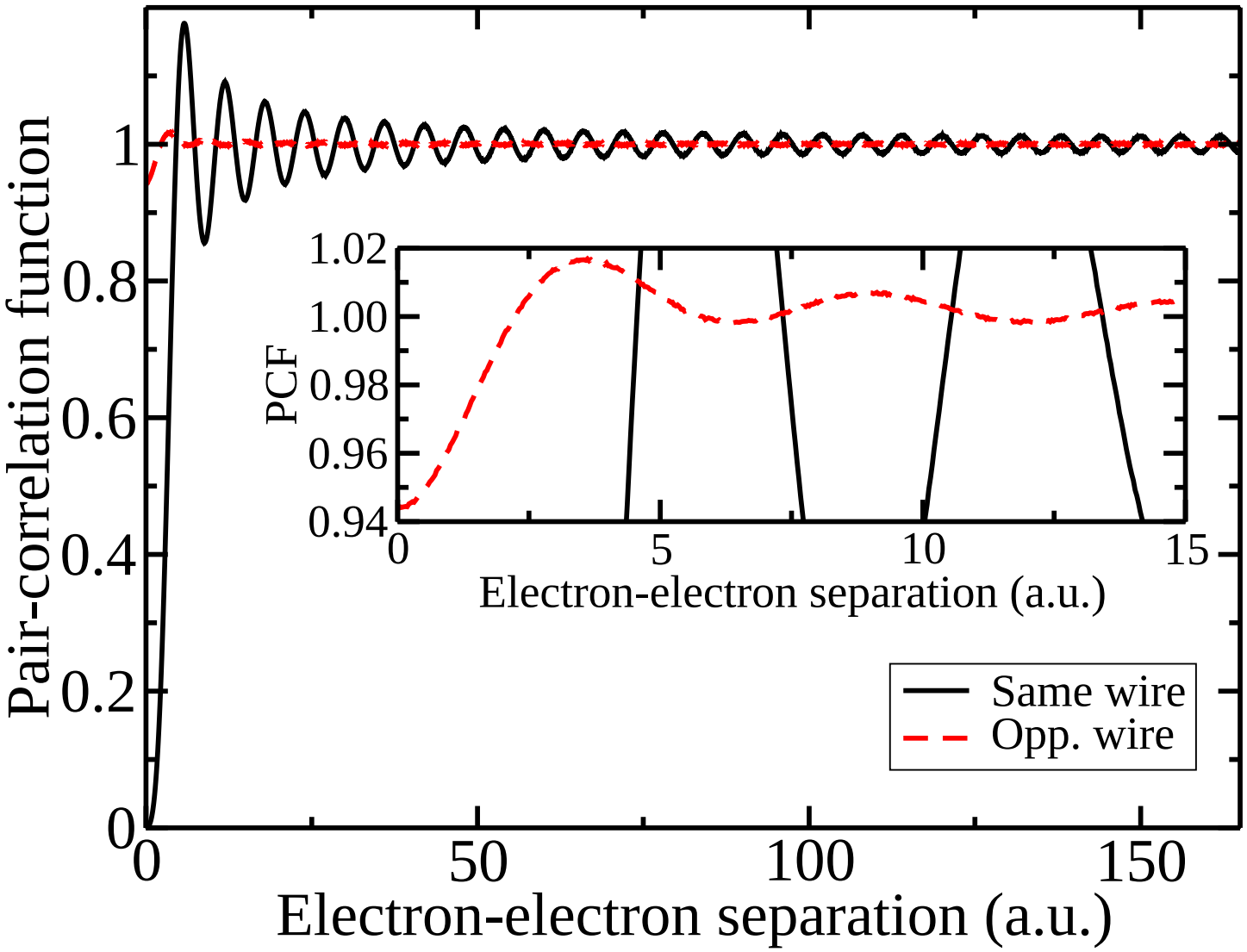


Biwire, $r_s = 3$ a.u., $z = 3$ a.u.

# Static Structure Factor of a Wire (I)

- The static structure factor $S(q)$ is related to the PCF $g(x)$ by

$$S(q) = 1 + n \int_{-\infty}^{\infty} [g(x) - 1] \exp(-iqx)\, dx,$$

  where $n = 1/(2r_s)$ is the number density.

- Experimentally accessible quantity.

- Calculate $S(q)$ by taking Fourier transform of fit to PCF.

- Single $\delta$-function peak in $S(q)$. Strongly correlated fluid phase.

- Would like to calculate the momentum distribution too.

# Static Structure Factor of a Wire (II)

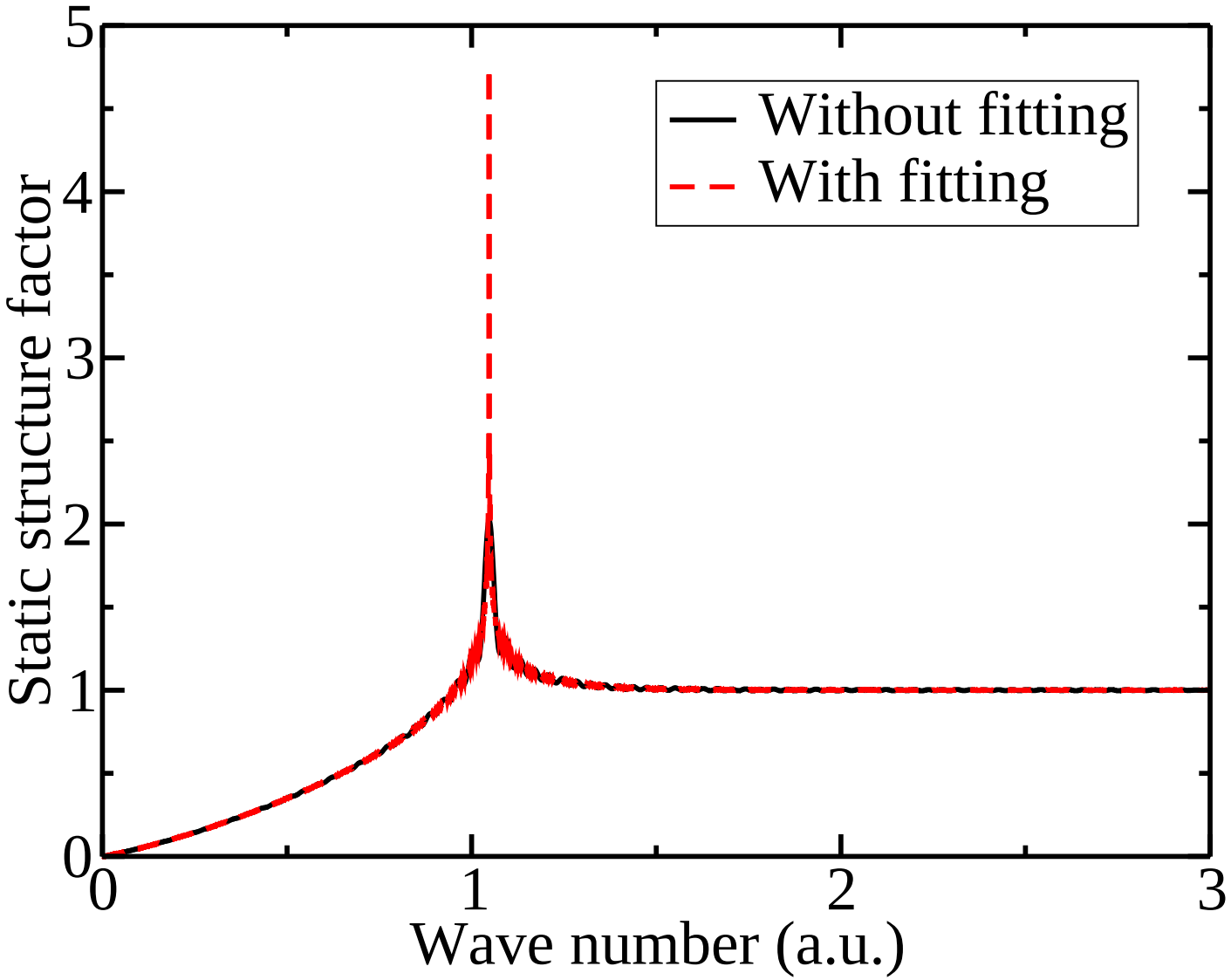


$r_s = 3$ a.u.; 55 electrons; VMC data

# Casimir Effect and van der Waals Binding

- At very large separations ($z > 70246 r_s^2$ within the RPA) the **Casimir effect** is the dominant source of attraction between thin, neutral metallic layers.[8]

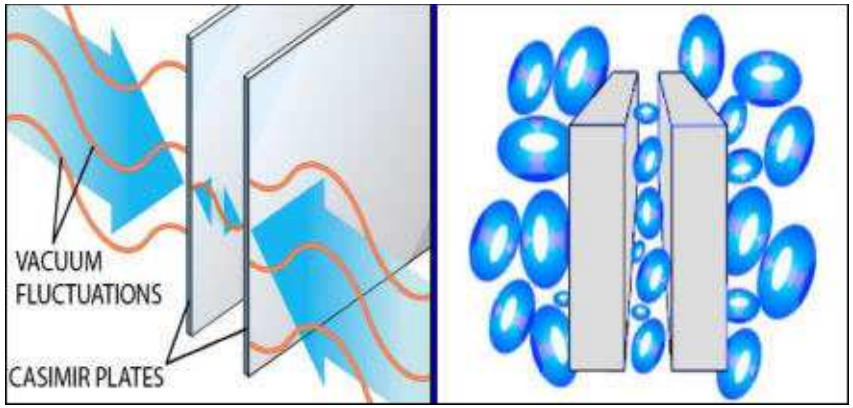


- The zero-point energy of photon modes between the layers depends on the separation; this results in an attractive force between the layers. Use QED to calculate.

- Casimir binding energy: $E_{\rm cas} = -c\pi^2/(720 z^3)$, where $c$ is the speed of light.

- We will only consider the regime in which van der Waals forces dominate, i.e. the regime described by the nonrelativistc many-electron Schrödinger equation.

[8] H. B. G. Casimir and D. Polder, Phys. Rev. **73**, 360 (1948); B. E. Sernelius and P. Björk, Phys. Rev. B **57**, 6592 (1998).

# Binding Energy of a Thin Metallic Bilayer (I)

- Standard theory: interaction between surface elements of area $\delta a_1$ and $\delta a_2$ separated by $r$ is $\alpha \delta a_1 \delta a_2 / r^6$, where $\alpha$ is a constant; so binding energy per particle is

$$U(z) = \frac{\pi r_s^2}{2} \int_{-\infty}^{\infty} \int_{-\infty}^{\infty} \frac{\alpha}{(x^2 + y^2 + z^2)^3} \, dx \, dy \sim z^{-4}.$$

- Is inevitable consequence of using Lennard-Jones potentials for bilayer.

- Clearly appropriate for an insulator. What about a conductor?

- RPA binding energy of a HEG bilayer is[9]

$$U(z) = \frac{-0.012562 \sqrt{\pi} r_s}{2 z^{5/2}}.$$

[9] B. E. Sernelius and P. Björk, Phys. Rev. B **57**, 6592 (1998).

# Binding Energy of a Thin Metallic Bilayer (II)

- As with biwire, perform DMC calculations (i) to verify asymptotic form predicted by RPA and (ii) to obtain the correct prefactor.
- "Capacitor energy" ($E_{\rm cap} = z/r_s^2$) must be added to our DMC energies.
- Expect large cancellation of finite-size effects when monolayer energy is subtracted from bilayer energy, so long as separation is less than simulation-cell length.
- Used Slater-Jastrow-backflow wave function at $r_s = 1$ a.u.; Slater-Jastrow wave function at other densities.
- Used time steps of 0.02 a.u., 0.05 a.u. and 0.5 a.u. and populations of 1024, 320 and 1024 configurations in our calculations at $r_s = 1$, 3 and 10 a.u., respectively.
- Verified that time-step bias is negligible at $r_s = 3$ and 3 a.u.by halving time step; monolayer & bilayer energies did not change significantly. Small time-step bias at $r_s = 10$, but even without cancellation of biases, it would not significantly affect the binding-energy graph.

# Binding Energy of a Metallic Bilayer (III): $r_s = 1$ a.u.

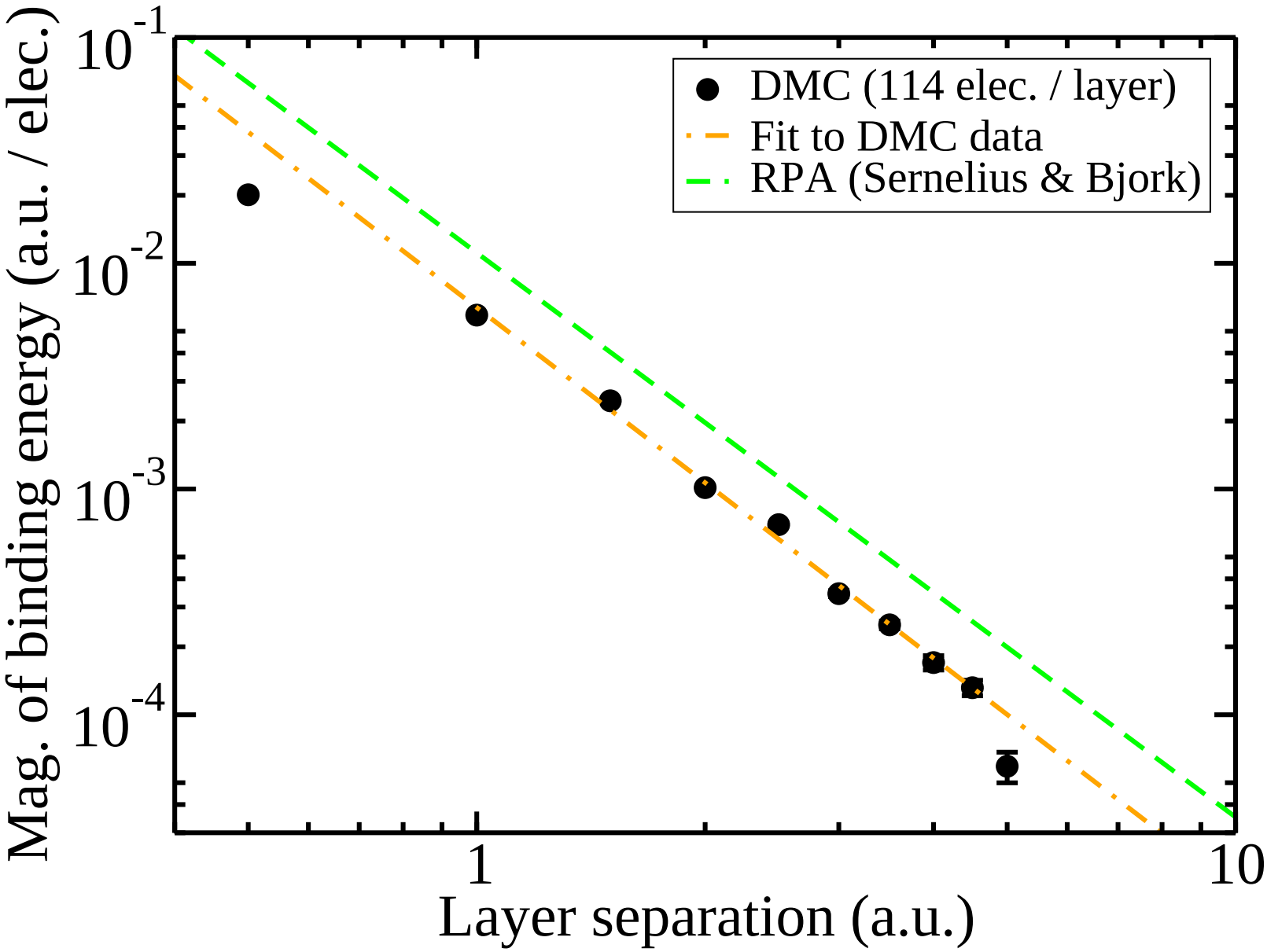

# Binding Energy of a Metallic Bilayer (III): $r_s = 3$ a.u.

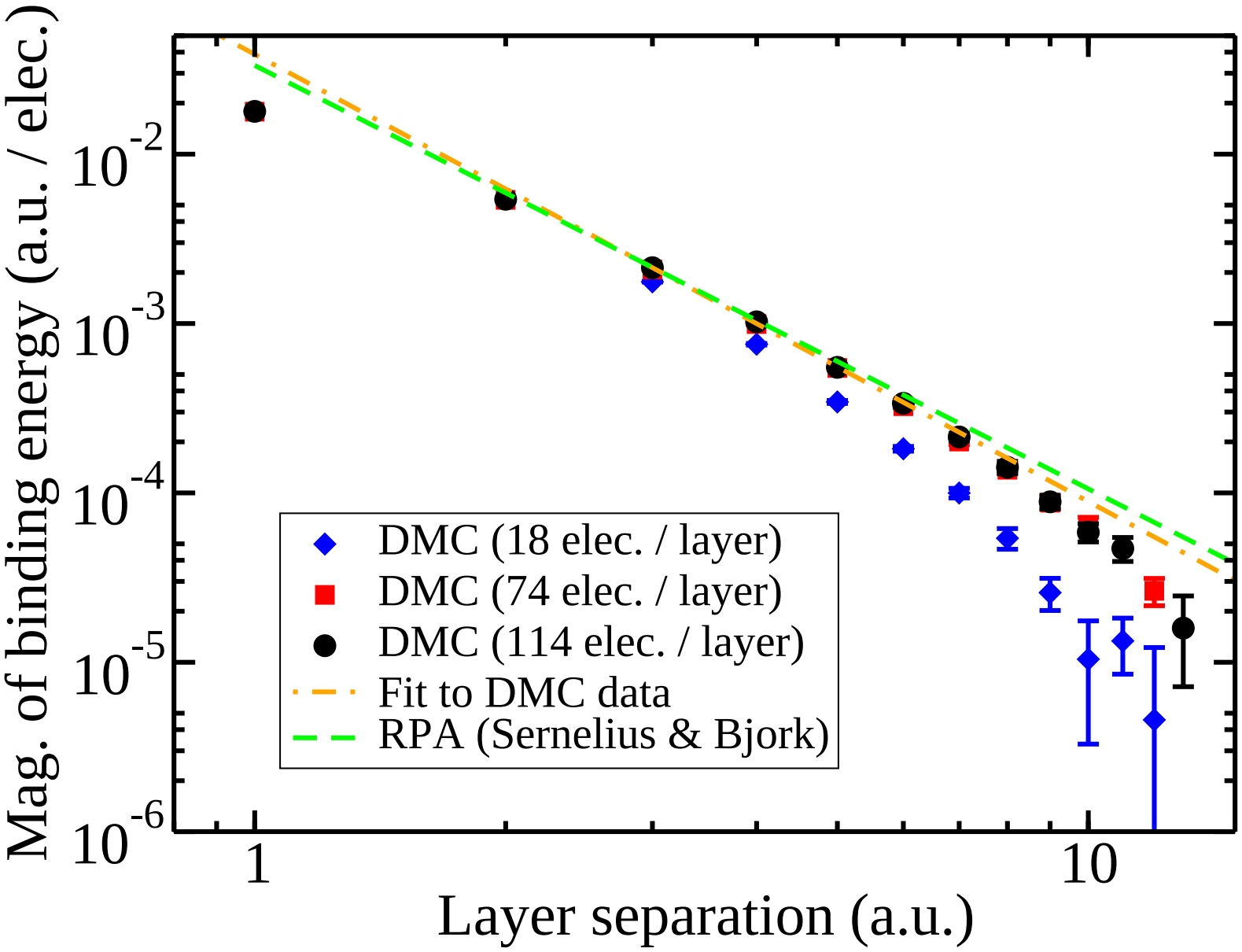

# Binding Energy of a Metallic Bilayer (III): $r_s = 10$ a.u.

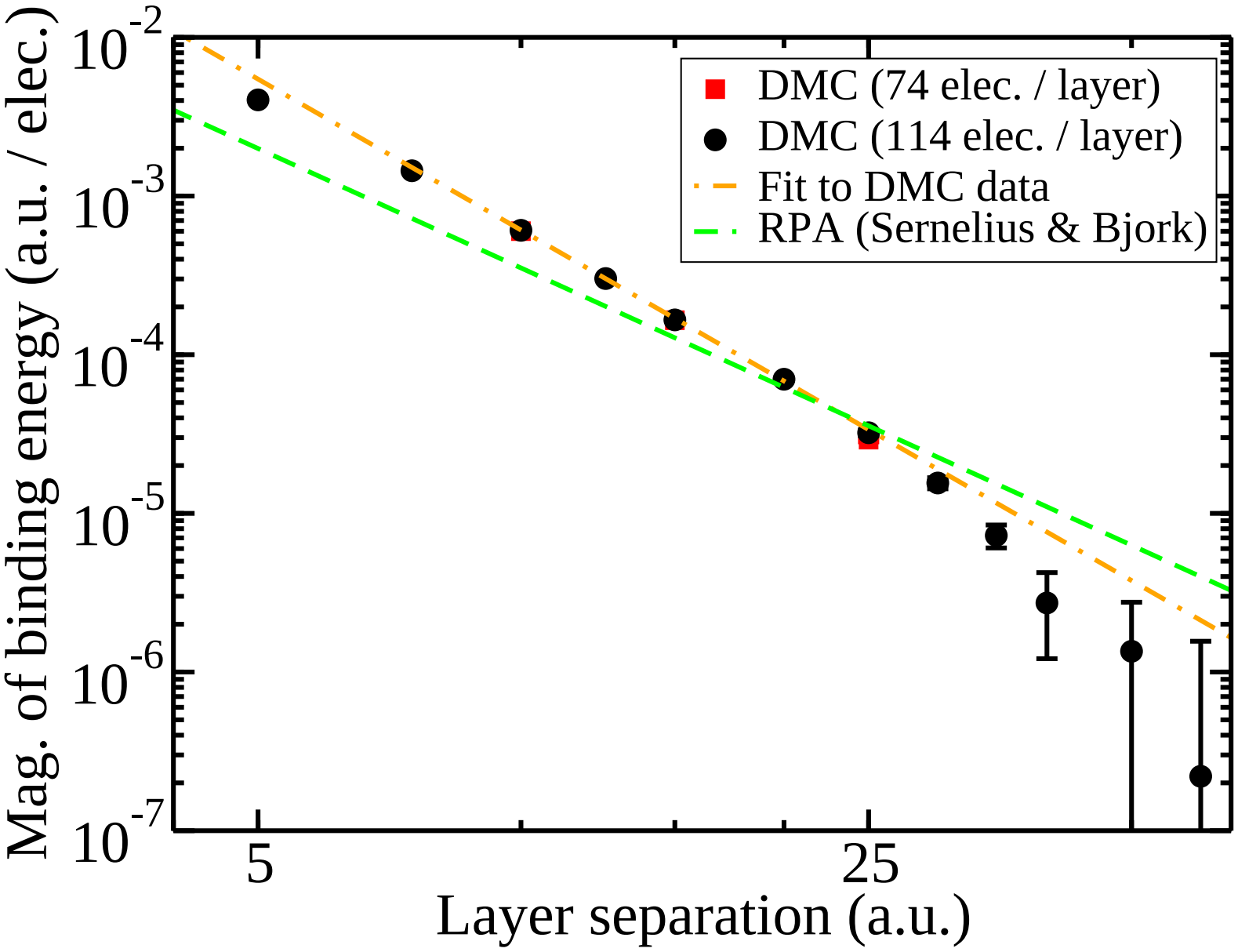

# Binding Energy of a Metallic Bilayer (IV)

| $r_s$ (a.u.) | Asymptotic binding energy (a.u. per electron) RPA | DMC |
|---|---|---|
| 1 | $-0.011133z^{-5/2}$ | $-0.00637z^{-2.58}$ |
| 3 | $-0.033398z^{-5/2}$ | $-0.0388z^{-2.64}$ |
| 10 | $-0.11133z^{-5/2}$ | $-0.882z^{-3.16}$ |

- The DMC binding energies are in broad agreement with the RPA predictions. They fall off much less rapidly than the $z^{-4}$ decay predicted by the standard theory.
- Uncertainties in exponents are about $0.1$–$0.2$.
- $r_s = 1$ a.u.: RPA gives correct behaviour but somewhat overestimates the prefactor.
- $r_s = 3$ a.u.: the DMC and RPA results are in good agreement.
- $r_s = 10$ a.u.: the DMC binding energy falls off more rapidly than the RPA binding energy. The RPA must be missing some important correlation effects at low density.

# Bilayer Pair-Correlation Functions

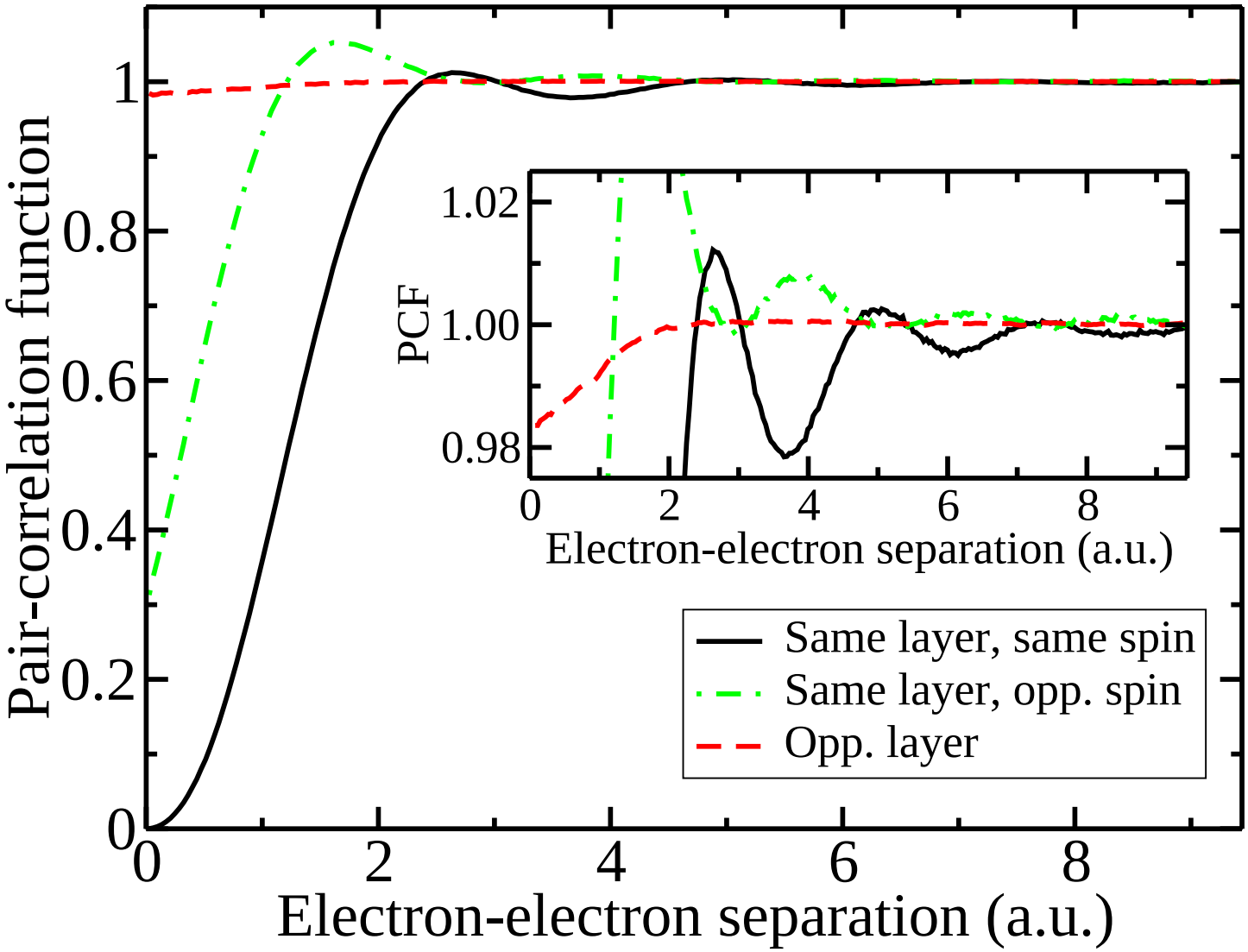


Bilayer, $r_s = 1$ a.u., $z = 2$ a.u., SJB wave function, extrapolated PCF

# Conclusions

- We have obtained accurate binding energies for pairs of thin, parallel, metallic layers and wires using DMC.

- Our results are in broad agreement with recent RPA calculations of the binding energy. *This confirms that the common practice of using Lennard-Jones pair potentials to describe the binding of metallic wires and layers is qualitatively incorrect.*

- Our data could be used to parametrise the wire–wire and layer–layer interaction potentials used in models of nanotechnological devices, or to generate van der Waals energy functionals for use in DFT calculations.

- Some differences between DMC and RPA: at low densities the DMC bilayer binding energy falls off more rapidly.

- We are obtaining DMC energy, pair-correlation-function and structure-factor data for a 1D HEG in the limit of zero wire thickness. ($Work\ in\ progress.$)

# Acknowledgements

We acknowledge financial support from Jesus College, Cambridge and the Engineering and Physical Sciences Research Council.



Computing resources were provided by the Cambridge High Performance Computing Service and HPCx.